



# Association of Fibrotic and Apoptotic Markers in Renal Tubulointerstitial Fibrosis Induced by Unilateral Ureteral Obstruction

Sahar Hamed<sup>1\*</sup>, Nashwa Barakat<sup>1</sup>, Mohamed Sobh<sup>1,2</sup>, Nahla Anber<sup>2</sup>, Basma Hamed<sup>3</sup> and Fatema Moustafa<sup>4</sup>

<sup>1</sup>Urology and Nephrology Center, Mansoura University, Mansoura, Egypt

<sup>2</sup>Department of Biochemistry, Emergency Hospital, Mansoura University, Mansoura, Egypt

<sup>3</sup>Medical Experimental Research Center, Faculty of Medicine, Mansoura University, Mansoura, Egypt

<sup>4</sup>Pathology Department, Faculty of Medicine, Mansoura University, Mansoura, Egypt

## Abstract

Many apoptotic and fibrotic markers are known to be important in the development of renal fibrosis. In Unilateral Ureteral Obstruction (UUO) the Obstructed Kidney (OK) develops fibrosis, while the Contralateral (CL) does not. In this study we investigated the gene expression of different apoptotic and fibrotic molecules which may affect fibrosis developments due to UUO. UUO was prepared under isoflurane anesthesia, and the animals were sacrificed after 3, 7 and 14 days post UUO. UUO caused hydronephrosis, dilation of renal tubules, loss of parenchymal thickness, apoptosis and fibrosis. Damage was most severe in mice sacrificed after 14 days of UUO, while both 3 and 7 days groups showed considerably milder hydronephrosis, no tubular necrosis, and less tubular dilation. We detected increased levels of transforming growth factor  $\beta$  (TGF- $\beta$ ) and alpha-smooth muscle actin ( $\alpha$ -SMA), Matrix metalloproteinase 2 (MMP2) and MMP9 (fibroblast activation marker) and TNF as apoptotic marker in the kidney tissue of UUO mice relative to the control UUO mice. This increase was confirmed by immunohistochemistry and gene expression as well. In conclusion, we found that the different pro-fibrotic molecules,  $\alpha$ -SMA, TGF- $\beta$ , MMP2, MMP9, Fibronectin and pro-apoptotic molecule, TNF expression were increased in UUO mouse kidney compared to contralateral or sham kidney. This increase was found to be time dependent.

**Keywords:** Tubulointerstitial injury; Fibrosis; Unilateral ureteral obstruction; Apoptotic markers; Fibrotic markers

## Introduction

Chronic Kidney Disease (CKD) is a public health problem worldwide [1,2]. Obstructive nephropathy is a common cause of kidney damage and renal insufficiency, both in congenital obstructive nephropathy in children [3], and acquired obstruction caused by kidney stones, malignancies and benign prostate hyperplasia [4]. Many factors are involved in the onset and progression of CKD. Renal tubulointerstitial fibrosis, characterized by ECM deposition, interstitial myofibroblast proliferation, and the infiltration of inflammatory mononuclear cells, is thought to play an important role in the pathogenesis of CKD [5].

Unilateral Ureteral Obstruction (UUO), a commonly used experimental model of chronic kidney injury is characterized by tubular atrophy, inflammation and interstitial fibrosis [6]. UUO is interesting both as a model of ureteral obstruction, and for studying the fibrotic process as such [7]. In UUO, the initiating damage is increased ureteral pressure transmitted retrograde to the kidney that causes secondary renal vasoconstriction and resultant reduced glomerular blood flow [8]. The development and degree of fibrosis is considered to be one of the most reliable prognostic markers for loss of kidney function and progression towards End Stage Renal Disease (ESRD) [9].

The resultant tubulointerstitial fibrosis in UUO is multi-factorial, including interstitial macrophages producing pro-inflammatory cytokines, tubular cells undergoing apoptosis, and resident renal cells transitioning to collagen-producing cells [8,10]. Renal fibrosis involves a complex network of cellular interactions, cytokine/chemokine production, and signaling pathways [8] the dysregulations of which may cause fibroblast activation [11,12], Epithelia to Mesenchymal Transition (EMT) [13,14] monocyte/macrophage infiltration [15], and cellular apoptosis [16] eventually leading to histological alterations in the kidney tissue.

Although much progress has been made, our understanding of the cellular and molecular mechanisms of interstitial fibrosis still remains uncompleted. The aim of the present study is to evaluate the association of fibrotic and apoptotic markers in renal tubulointerstitial fibrosis induction using unilateral ureteral obstruction mouse model.

## Materials and Methods

### Animals and UUO

C57/BL6 mice ~6 weeks old were purchased from the (Charles River Laboratory, France) bred and maintained in Mansoura Experimental Research Center (MERC), Faculty of Medicine, Mansoura University. Experiments were carried out in accordance with the protocols approved by the Animal Ethics Committee of Mansoura University. Kidney fibrosis was induced by UUO as previously described [2]. Briefly, mice were anesthetized with isoflurane (1%, inhaled). UUO was induced by left ureteral ligation using a 6-0 silk tie suture at two points. Sham-operated mice underwent the same surgical procedure except for the ureteral ligation. After 3, 7 or 14 days of UUO or sham operation, the mice were sacrificed and renal tissues were harvested.

**\*Corresponding author:** Sahar Hamed, Professor of Immunology and Molecular Biology, Urology and Nephrology Center, Mansoura University, Mansoura, Egypt, Tel: +2 (012) 2665-3597; E-mail: [saharmhamed@gmail.com](mailto:saharmhamed@gmail.com)

**Received:** February 12, 2019; **Accepted:** April 19, 2019; **Published:** April 30, 2019

**Citation:** Hamed S, Barakat N, Sobh M, Anber N, Hamed B, et al. (2019) Association of Fibrotic and Apoptotic Markers in Renal Tubulointerstitial Fibrosis Induced by Unilateral Ureteral Obstruction. J Biomed Pharm Sci 2: 124

**Copyright:** © 2019 Hamed S, et al. This is an open-access article distributed under the terms of the Creative Commons Attribution License, which permits unrestricted use, distribution, and reproduction in any medium, provided the original author and source are credited.

The kidneys were cut in transverse slices that were stabilized in RNA-later, or fixed in 4% formaldehyde, processed and embedded in paraffin.

### Immunohistochemistry

For immunohistochemical staining, the sections were deparaffinized with xylene, rehydrated by increasing concentrations of alcohol and rinsed for 10 min in 0.1 M PBS. After that, the sections were treated with 0.02% hyaluronidase in PBS for 20 min at 37°C for antigen retrieval and immersed in 0.3% methanol containing 1% hydrogen peroxide for 30 min to block endogenous peroxidase and rinsed in 0.05 M PBS plus 0.025% Triton X-100 for 10 min at room temperature. Then, the sections were incubated in 10% normal goat serum with 1% BSA in PBS for 30 min at room temperature. Subsequently, all sections were covered with the primary antibody of  $\alpha$ -SMA (VP-S281, VECTOR Laboratories, CA, USA), metalloproteinase 2 (MMP2) (SA-616-0050, ENZO Life Science, USA), and Transforming Growth Factors- beta (TGF- $\beta$ ) antibody (5559-100, BioVision, CA, USA), collagen III (Rabbit IgG polyclonal, Abcam, ab6310, USA) or tumor necrosis factor-  $\alpha$  (TNF-  $\alpha$ ) (sc-130220; Santa Cruz Biotechnology, USA) and incubated overnight at 4°C. Sections were then incubated with secondary antibody (SK-4100, VECTOR Laboratories, CA, USA) for 1 h at room temperature. After staining, the sections were randomly chosen to estimate positively stained area. The sections were counterstained with Mayer's hematoxylin and finally were dehydrated in increasing concentrations of alcohol, cleared in xylene and mounted.

In order to detect staining intensity, the reactions of the tested antibody (five slides for each stage) were observed by three examiners blindly with Olympus microscope (AH-2, Japan). On the basis of their staining intensity, the sections were graded as very weak (+), weak (++), moderate (+++) and strong (++++). The immunoreactive specificity was checked by negative and positive controls as follows:

1. Negative control: a control incubated with normal mouse serum instead of the primary antibody
2. Positive control: Positive organ of the corresponding antigen was incubated with antibodies overnight at 4°C.

### Special stain staining

Conventional staining for all groups using Hematoxylin & Eosin was done evaluating the morphometric interstitial changes and fibrosis as well. Different morphometric changes were observed like, glomerular infiltration rate, interstitial inflammation, interstitial fibrosis, and dilated tubules. For Masson trichrome staining, the 4  $\mu$ m slides were stained by routine procedures. The blue staining area represented the fibrosis. For Periodic Acid Sheiff, the red staining area represented the precipitated collagen in basement membrane. Each morphometric change was scored as weak (+), moderate (++) and strong (+++) for statistical analysis.

### RNA extraction and quantitative real time PCR

Total RNA extraction from kidney tissue was conducted using Trizol reagent (Invitrogen, USA) in compliance with the manufacturer's instructions. The total RNA was used for cDNA synthesis with the High-Capacity Reverse Transcription Kit (Applied Biosystems, USA). Real-time PCR was performed following a standard protocol on the ABI 7900HT System (Applied Biosystems, USA). The relative expression levels of TNF  $\alpha$ -SMA, MMP2, MMP9 and Fibronectin were normalized to the internal control (GAPDH). The specificity of real-time PCR was confirmed *via* routine agarose gel electrophoresis and Melting-curve

analysis. The primers for TNF  $\alpha$ -SMA, MMP2, MMP9, Fibronectin and GAPDH cDNA amplification are listed in Table 1.

### Statistical analysis

Data is presented as means  $\pm$  Standard Error of the Mean (SEM), except for comparison of the expression of individual genes where the fold-change is used. The probability of chance difference was tested using ANOVA, with Fisher's test and *a priori* contrasts to test individual comparisons.  $P < 0.05$  was accepted as statistically significant.

## Results

### Morphometric evaluation of interstitial fibrosis

By applying one way ANOVA test through the different UO sacrifice time for morphometric evaluation of interstitial fibrosis a significant analysis both between and within groups for glomerular infiltration, interstitial inflammation, interstitial fibrosis, necrosis, apoptosis and dilated tubules. The same observation was conducted with special stains as MT which representing fibrosis, PAS representing glycogen precipitate as well as immunohistochemical stains for TNF representing apoptosis,  $\alpha$ -SMA, MMP2 and TGF- $\beta$  as pro-fibrotic markers as well as collagen III representing fibrosis.

By applying student-T test between different UO groups and normal control group, in H&E stained slides, a highly significant increase throughout UO sacrifice time for morphometric evaluation in glomerular infiltration, interstitial inflammation, interstitial fibrosis, necrosis, apoptosis and dilated tubules. Table 2 representing different

Transcript		Primer Sequence
TNF	F	5'- CAGGCGGTGCCTATGTCTC-3'
	R	5'- CGATCACCCCGAAGTTCAGTAG-3'
$\alpha$ -SMA	F	5'- ACTGGGACGACATG-GAAAAG-3'
	R	5'- CATCTCCAGAGTCCAGCACA-3'
MMP2	F	5'- GCGGCGGTCACAGTACTT-3'
	R	5'- CAGCTCTTCAGACTTTGGTTCT-3'
MMP9	F	5'- TGGGGGGCAACTCGGC-3'
	R	5'- GGAATGATCTAAGCCAG-3'
Fibronectin	F	5'- AT-GATGAGGTGCACGTGTGT-3'
	R	5'- TCTCCAGAGTCACCAATC-3'
GAPDH	F	5'- AGGTCGGTGTGAACGGATTG-3'
	R	5'- GGGGTCGTTGATGGCAACA-3'

Table 1: Primers used for real-time PCR.

Group	G Infiltrate	Int. Inflamm.	Int. Fibrosis	Necrosis	Dilated Tub
<b>C</b>					
M	1.00	1.00	1.00	1.00	1.00
SE	0.01	0.01	0.01	0.01	0.01
<b>3 Days</b>					
M	1.83	1.83	1.83	3.33	2.83
SE	0.408	0.408	0.408	0.816	1.169
p	0.020	0.020	0.020	0.0001	0.011
<b>7 Days</b>					
M	1.17	1.50	1.33	3.67	3.00
SE	0.408	0.548	0.516	0.816	1.265
p	0.020	0.020	0.0001	0.0001	0.001
<b>14 Days</b>					
M	3.17	3.83	3.50	3.83	2.50
SE	0.983	0.408	0.548	0.408	1.225
p	0.0001	0.0001	0.0001	0.0001	0.0001

G Infiltrate: Glomerular Infiltration; Int. Inflamm: Interstitial inflammation; Int. Fibrosis: Interstitial fibrosis; Dilated Tub: Dilated tubules.

Table 2: Statistical analysis of morphometric parameters evaluating interstitial fibrosis between different UO groups compared to control group.

morphometric parameters evaluating interstitial fibrosis between different UUO groups compared to control group. After 3 days post operation, the kidney shows hypercellularity of mesangial cells with marked lymphohistiocytic exudate in interstitial tissue, dilation of renal glomeruli, interstitial nephritis with fibroblastic proliferation. Kidney shows degenerative change in renal tubules with histiocytic infiltrations in interstitial tissue, severe congestion in interstitial blood capillaries with cystic dilatation of renal tubules and loss of renal tubules Figures 1 and 2.

After 7 days post operation, the kidney shows lymphohistiocytic exudate infiltrate interstitial tissue with mild fibroblastic proliferation and cystic dilation of renal tubules, hypercellularity of activated mesangial cells with dissolution of renal glomeruli, proliferative glomerulonephritis with formation of epithelial crescent and congestion of glomerular capillaries, marked hemorrhage in interstitial tissue.

Although kidney shows mononuclear cell infiltrates the interstitial tissue with fibroblastic proliferation Figures 1 and 2.

After 14 days post operation, there is massive lymphohistiocytic infiltration interstitial tissue with replacement of the renal parenchyma, extensive replacement of renal tissue with chronic inflammatory exudate and fibroblastic proliferation in interstitial tissue with degeneration of the renal parenchyma Figures 1 and 2.

By using special stains at different UUO sacrifice time. MT representing fibrosis developed by blue color as Special stain, which shows different color intensities according to the fibrosis degree Figures 3 a-d. A highly significant increase was noted throughout UUO sacrifice time for fibrosis as representing with the degree of blue color in MT stain. Glycogen precipitated in basement membrane stained by PAS (special stain) representing by red color Figures 3 e-h. A highly

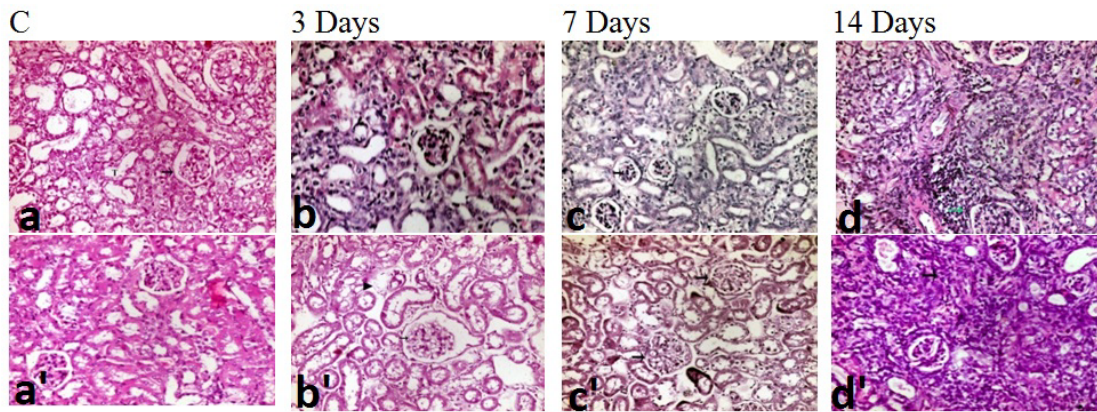


**Figure 1:** Morphometric changes in different UUO groups and control group (HE, 400 X). **a, a')** Normal renal corpuscle (arrow) and tubules (T) Lined by cuboidal to columnar epithelium; **b)** Normal tubular epithelium with mild hypercellularity of mesangial cells; **b')** Dilation of renal glomeruli (arrow) and loss of renal tubules (arrow head); **c)** Hypercellularity of activated mesangial cells with dissolution of renal glomeruli (arrow); **c')** Proliferative glomerulonephritis with formation of epithelial crescent (arrow); **d)** Extensive replacement of renal Tissue with chronic inflammatory exudates and fibroblastic proliferation (arrow); **d')** Fibroblastic proliferation in interstitial tissue (arrow) with degeneration of the renal parenchyma.

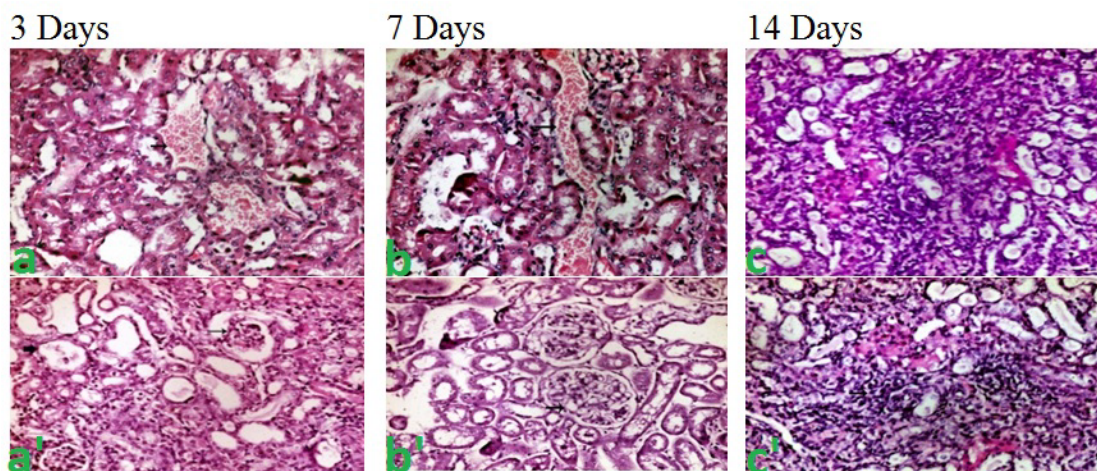


**Figure 2:** Morphometric changes in different UUO groups and control group (HE, 400 X). **a)** Severe congestion in interstitial blood capillaries (arrow) with cystic dilatation of renal tubules, **a')** Dissolution of renal glomeruli (arrow) and degeneration of the renal tubules (thick arrow), **b)** Marked hemorrhage in interstitial tissue (arrow); **b')** Proliferative glomerulonephritis with congestion of glomerular capillaries (arrow); **c)** Round cell infiltrations in interstitial tissue (arrow) with replacement of the renal parenchyma; **c')** Necrosis of renal tubules with lymphohistiocytic exudates in interstitial tissue and fibroblastic proliferation (arrow).

significant increase was noted throughout UUO sacrifice time for glycogen precipitate as representing with the degree of red color in PAS stain.

Using immunohistochemical stain at different UUO sacrifice time, different markers were stained as  $\alpha$ -SMA, MMP2 and TGF- $\beta$  as pro-fibrotic markers Figure 4 as well as collagen III representing fibrosis and TNF representing apoptosis Figure 5. A highly significant increase was

noted throughout UUO sacrifice time was noted for different markers stained as representing with the degree of brown stain.

### Genetic evaluation of interstitial fibrosis

By evaluating gene expression for TNF  $\alpha$ -SMA, MMP2, MMP9 and Fibronectin in UUO kidneys as well as Contralateral (CL) kidney as pro-fibrotic and apoptotic markers Figure 6, the up-regulation was noted in all markers evaluated when compared to the control or sham

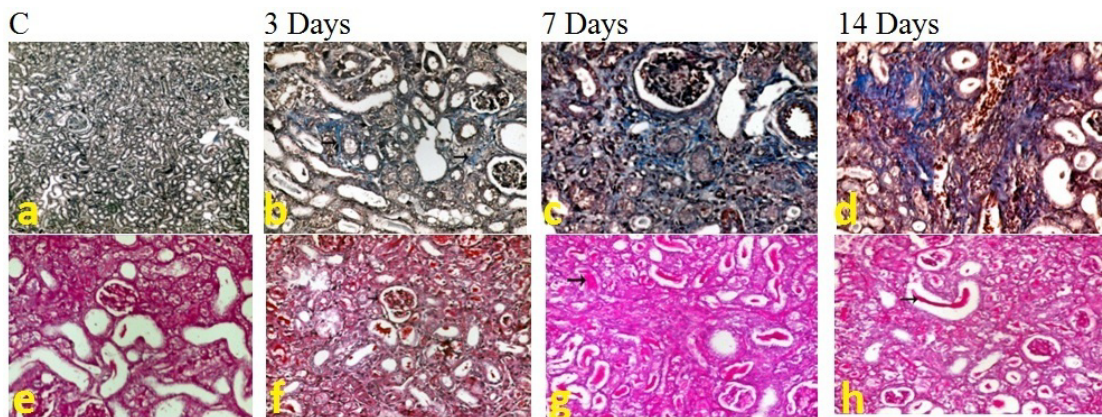


**Figure 3:** Representing special stain for the kidney of different UUO groups and control group (MT, a- d; PAS, e-h; 400 X). **a)** Normal kidney with no evidence of fibrous tissue deposition in renal parenchyma; **b)** mild fibrous tissue stained blue in interstitial tissue; **c)** moderate fibrous tissue stained blue in interstitial tissue; **d)** extensive fibrous tissue proliferation stained blue. **e)** Normal kidney with no evidence of glycogen deposition in renal tubules or thickening of basement membranes; **f)** mild stained thickened basement membrane of renal glomeruli (arrow); **g)** moderate reddish stained casts in the lumen of renal tubules (arrow) with fibrous tissue stained red in interstitial tissue; **h)** extensive reddish stained casts in the lumen of renal tubules.

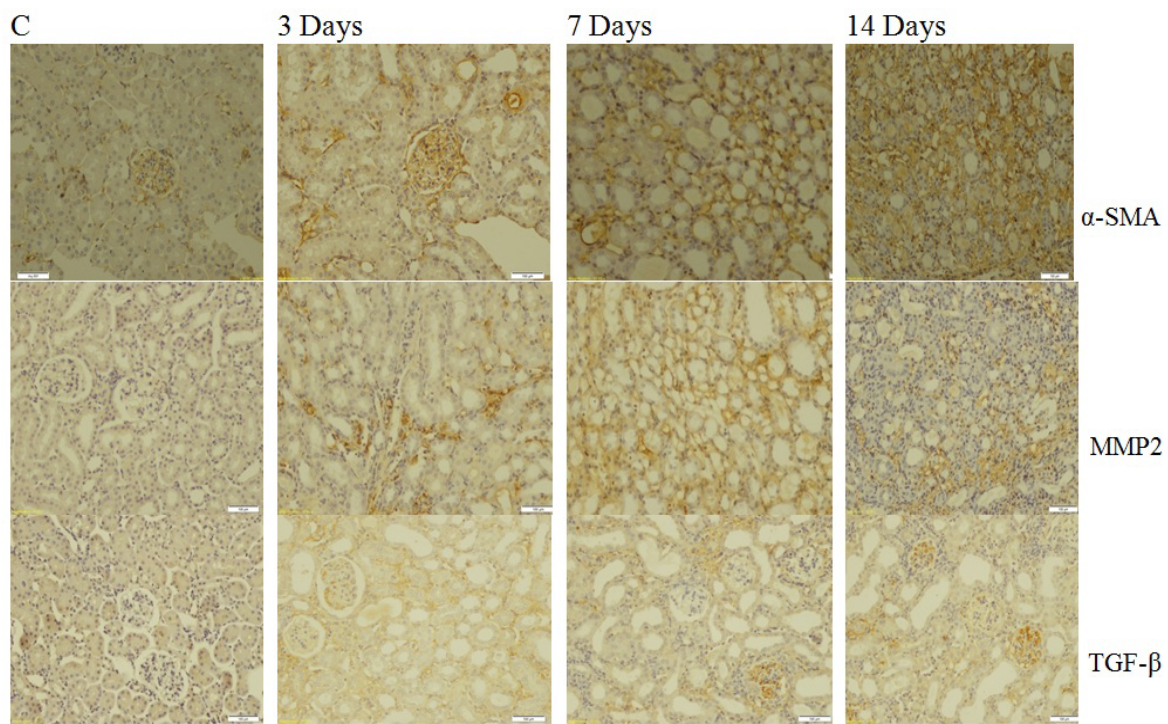


**Figure 4:** Representing immunohistochemical stain at different UUO sacrifice time showing different markers such  $\alpha$ -SMA, MMP2 and TGF- $\beta$  as pro-fibrotic markers (400 X).

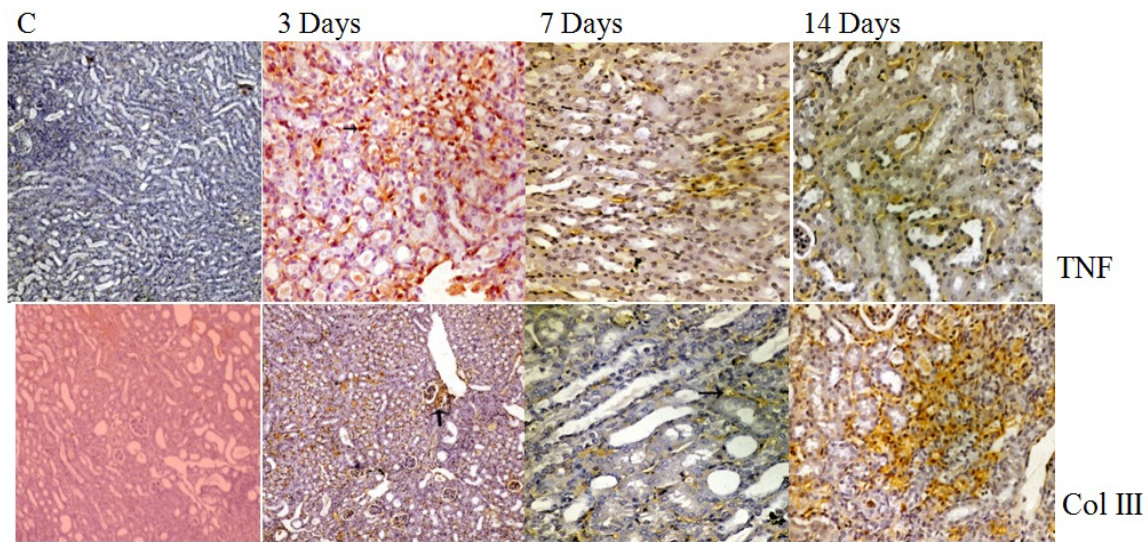


**Figure 5:** Representing immunohistochemical stain at different UO sacrifice time showing different markers such collagen III representing fibrosis and TNF representing apoptosis (400 X).

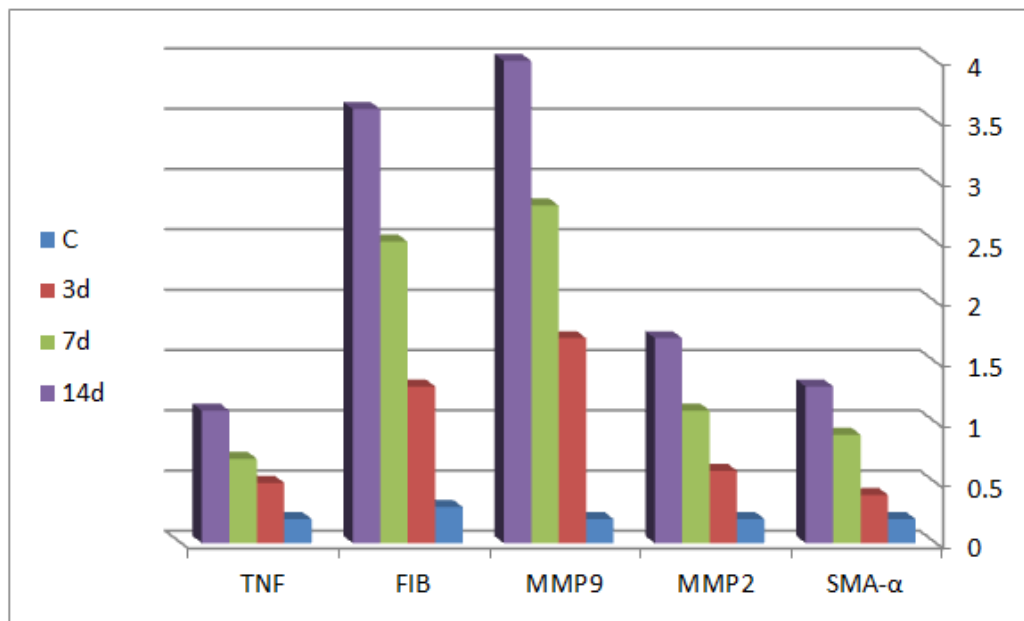


**Figure 6:** Real-time PCR shows TNF  $\alpha$ -SMA, MMP2, MMP9 and Fibronectin which normalized to the internal control (GAPDH), mRNA expression was performed in the control and different time UO mice kidneys. Total renal RNA extracted from kidneys was reverse-transcribed and subjected to real-time PCR, each bar represents the mean  $\pm$  SEM for a group of five mice.

group kidneys. This up-regulation was increase as the time of UO increase ( $p < 0.001$ ).

## Discussion

In the present study, we examine the involvement of some fibrotic and apoptotic markers in renal tubulointerstitial fibrosis induced by unilateral ureteral obstruction. Our results demonstrated that progressive tubulointerstitial fibrosis and apoptosis was increased as the UO time increased. UO is characterized by interstitial vascular loss

and progressive kidney fibrosis. The compensatory mechanisms that might attempt to counter these events are not well understood.

UO model of kidney fibrosis is a well-studied model for fibrosis evolution in mice kidneys. The obstruction of the ureter increases tubular pressure, reduces glomerular filtration rate, and activates many vasoactive hormones and cytokines through the kidney leading to fibrosis over time. The increasing amount of collagen as the disease progresses can be quantified by staining, immunohistochemistry or second harmonic generation microscopy [17,18].

Progressive tubulointerstitial fibrosis is the final common pathway for all kidney diseases leading to chronic renal failure [2]. Renal interstitial fibrosis typically resulted from chronic inflammation through production of related molecules, such as angiogenic factors, growth factors, fibrogenic cytokines and proteinase [19]. Renal inflammation is a universal response to infectious and noninfectious triggers. Non-microbial inflammation is an important component of many acute and chronic renal diseases [20,21].

In UUO mice model the kidney with the obstruction develops extensive fibrosis over time. The increase in fibrosis is dependent on the time of UUO. Amount of collagen fibers increases over time and tissue architecture also undergoes progressively more changes [17]. Thus the lifetime signature and hence phasor distribution changes increasingly as time of UUO continues. A second hypothesis is that over time there are changes in the tissue architecture in comparatively Contralateral (CL) kidney also. In absence of a fully functional of obstructed kidney, healthy kidney of an UUO animal is used more than the obstructed kidney of a fully healthy mouse (hyperfiltration, etc.). Thus overtime the Contralateral (CL) kidney can also become diseased.

As it has long been recognized,  $\alpha$ -SMA is an indicative marker for myofibroblasts activation. Although it's precise origin is diverse and still controversial [22] myofibroblast remains the main effector cells during renal fibrogenesis. In an attempt to further clarify the role and associated cascades of both apoptotic and fibrotic markers in renal fibrosis, we performed UUO on C57/BL6 mice as animal model of tubulointerstitial fibrosis. Our current data demonstrated that  $\alpha$ -SMA, TGF- $\beta$ , MMP2, MMP9, Fibronectin as pro-fibrotic molecules as well as TNF as pro-apoptotic molecules expression were increased in UUO mouse kidney compared to contralateral or sham kidney. Our results are in accordance with previous studies [10,14,18].

MMP2 cleaves type IV collagen, and degrades already denatured collagens. The reduced MMP2 expression during UUO protects mice against hydronephrosis and renal fibrosis as indicated by both histology and gene expression in MMP2 in mutant mice [10]. The genetic mechanism seems to be a reduced ability to respond with MMP2 up-regulation under stress, and this may suggest that there is a threshold level of MMP2 necessary for pelvic remodelling and genetic events leading to activation of fibrosis. Endothelial cells are known to contribute to kidney fibrosis *via* Endothelial-Mesenchymal Transition (EndoMT). A study demonstrates that MMP-9-dependent signaling plays an important role in kidney fibrosis through EndoMT of Primary Mouse Renal Peritubular Endothelial Cells (MRPECs) [14]. The MMP-9 biological functions are depending on its cellular origins and site of activity. MMP-9 of both tubular and macrophage origin was critical to TGF- $\beta$ 1 induced tubular cell EMT [23]. It has been confirmed that MMP-9 is necessary for the disruption of epithelial cell basement membrane, a key step to complete the entire course of EMT [14]. Kidney endothelial cells that underwent EndoMT were recently demonstrated to play a more important role in kidney fibrosis than tubular cells or pericytes [24]. But the underlying molecular mechanism remains poorly defined. Their results demonstrated that MMP-9 indeed mediates TGF- $\beta$ 1-induced EndoMT, *via* activation of the Notch pathway [14].

## Conclusion

In summary, we found that the different pro-apoptotic molecules,  $\alpha$ -SMA, TGF- $\beta$ , MMP2, MMP9, Fibronectin and pro-apoptotic molecule, TNF expression were increased in UUO mouse kidney compared to contralateral or sham kidney. This may indicate that

these markers have plays an important role in kidney fibrosis, at least partly through EndoMT of peritubular endothelial cells. The increased expression in these markers was shown to be increased as well with time. This model was found to be a good model to study different approaches to prevent kidney fibrosis.

## Acknowledgement

This work was supported by the Science and Technology Development Fund (STDF) Project Grants number (1067).

## References

1. Levey AS, Atkins R, Coresh J, Cohen EP, Collins AJ, et al. (2007) Chronic kidney disease as a global public health problem: approaches and initiatives-a position statement from Kidney Disease Improving Global Outcomes. *Kidney Int* 72: 247-259.
2. Ke Y, Tang H, Ye C, Lei CT, Wang YM, et al. (2016) Role and Association of Inflammatory and Apoptotic Caspases in Renal Tubulointerstitial Fibrosis. *Kidney Blood Press Res* 41: 643-653.
3. Heikkilä J, Holmberg C, Kyllönen L, Rintala R, Taskinen S (2011) Long-term risk of end stage renal disease in patients with posterior urethral valves. *J Urol* 186: 2392-2396.
4. Hamdi A, Hajage D, Van Glabeke E, Belenfant X, Vincent F, et al. (2012) Severe postrenal acute kidney injury, post-obstructive diuresis and renal recovery. *BJU Int* 110: E1027-1034.
5. Zeisberg M, Neilson EG (2010) Mechanisms of tubulointerstitial fibrosis. *J Am Soc Nephrol* 21: 1819-1834.
6. Chevalier RL, Forbes MS, Thornhill BA (2009) Ureteral obstruction as a model of renal interstitial fibrosis and obstructive nephropathy. *Kidney Int* 75: 1145-1152.
7. Ucero AC, Benito-Martin A, Izquierdo MC, Sanchez-Niño MD, Sanz AB, et al. (2014) Unilateral ureteral obstruction: beyond obstruction. *Int Urol Nephrol* 46: 765-76.
8. Duffield JS (2014) Cellular and molecular mechanisms in kidney fibrosis. *J Clin Invest* 124: 2299-2306.
9. Nangaku M (2004) Mechanisms of tubulointerstitial injury in the kidney: final common pathways to endstage renal failure. *Intern Med* 43: 9-17.
10. Tveitars MK, Skogstrand T, Leh S, Helle F, Iversen BM, et al. (2015) Matrix Metalloproteinase-2 Knockout and Heterozygote Mice Are Protected from Hydronephrosis and Kidney Fibrosis after Unilateral Ureteral Obstruction. *PLoS ONE* 10: e0143390.
11. Mack M, Yanagita M (2015) Origin of myofibroblasts and cellular events triggering fibrosis. *Kidney Int* 87: 297-307.
12. Pan B, Liu G, Jiang Z, Zheng D (2015) Regulation of renal fibrosis by macrophage polarization. *Cell Physiol Biochem* 35: 1062-1069.
13. Inoue T, Umezawa A, Takenaka T, Suzuki H, Okada H (2015) The contribution of epithelial-mesenchymal transition to renal fibrosis differs among kidney disease models. *Kidney Int* 87: 233-238.
14. Zhao Y, Qiao X, Tan TK, Zhao H, Zhang Y, et al. (2017) Matrix metalloproteinase 9-dependent Notch signaling contributes to kidney fibrosis through peritubular endothelial-mesenchymal transition. *Nephrol Dial Transplant* 32: 781-791.
15. Meng XM, Nikolic-Paterson DJ, Lan HY (2014) Inflammatory processes in renal fibrosis. *Nat Rev Nephrol* 10: 493-503.
16. Zhou Y, Xiong M, Niu J, Sun Q, Su W, et al. (2014) Secreted fibroblast-derived miR-34a induces tubular cell apoptosis in fibrotic kidney. *J Cell Sci* 127: 4494-4506.
17. Ranjit S, Dvornikov A, Levi M, Furgeson S, Gratton E (2016) Characterizing fibrosis in UUO mice model using multiparametric analysis of phasor distribution from FLIM images. *Biomedical Opti Express* 7: 3519-3530.
18. Stefanska A, Eng D, Kaverina N, Pippin JW, Gross KW, et al. (2016) Cells of renin lineage express hypoxia inducible factor 2 $\alpha$  following experimental ureteral obstruction. *BMC Nephrol* 17: 5.

19. Sutariya B, Jhonsa D, Saraf MN (2016) TGF- $\beta$ : the connecting link between nephropathy and fibrosis. *Immunopharmacol Immunotoxicol* 38: 39-49.
20. Segelmark M, Hellmark T (2010) Autoimmune kidney diseases. *Autoimmun Rev* 9: A366-371.
21. Park JS, Kim S, Jo CH, Oh IH, Kim GH (2014) Effects of dietary salt restriction on renal progression and interstitial fibrosis in adriamycin nephrosis. *Kidney Blood Press Res* 39: 86-96.
22. Sato M, Muragaki Y, Saika S, Roberts AB, Ooshima A (2003) Targeted disruption of TGF-beta1/Smad3 signaling protects against renal tubulointerstitial fibrosis induced by unilateral ureteral obstruction. *J Clin Invest* 112: 1486-1494.
23. Tan TK, Zheng G, Hsu TT, Lee SR, Zhang J, et al. (2013) Matrix metalloproteinase-9 of tubular and macrophage origin contributes to the pathogenesis of renal fibrosis via macrophage recruitment through osteopontin cleavage. *Lab Invest* 93: 434-449.
24. LeBleu VS, Taduri G, O'Connell J, Teng Y, Cooke VJ, et al. (2013) Origin and function of myofibroblasts in kidney fibrosis. *Nat Med* 19: 1047-1053.